Available online at www.sciencedirect.com

SciVerse ScienceDirect

Ceramics International 39 (2013) 5845–5854

CERAMICS INTERNATIONAL

www.elsevier.com/locate/ceramint

Conventional and spark-plasma sintering of cordierite powders synthesized by sol–gel methods

Nozhat Moftah El-Buaishi[a], Djordje Veljović[a], Bojan Jokić[a], Željko. Radovanović[a], Ints Steins[b], Djordje Janaćković[a], Rada Petrović[a,*]

[a]*Faculty of Technology and Metallurgy, University of Belgrade, Karnegijeva 4, 11120 Belgrade, Serbia*
[b]*Institute of Inorganic Chemistry, Riga Technical University, Miera 34, Salaspils, LV-2169, Riga, Latvia*

Received 18 September 2012; received in revised form 18 December 2012; accepted 20 December 2012
Available online 11 January 2013

Abstract

Cordierite powders synthesized by colloidal and alkoxide sol–gel methods were conventionally and spark-plasma sintered. The powders for the sintering investigations were obtained by calcination of the gels at a temperature where α-cordierite is formed (crystalline powders) or at a temperature where densification without crystallization of silica-containing component occurred (amorphous powders). All the calcinated gels were ground for 3 h, uniaxial pressed at 400 MPa and sintered conventionally at 1400, 1430 and 1450 °C for 2 h. In order to improve the sintering behavior of the cordierite powders, spark-plasma sintering (SPS) was applied. The microstructures and the phase composition of the obtained cordierite materials were analyzed using scanning electron microscopy (SEM) and X-ray diffraction analysis and the mechanical properties of the materials were determined. It was shown that the sinterability of the colloidal powders was much better than that of the alkoxide powders. Conventional sintering at 1400 °C of the crystalline powder produced by the colloidal method gave the material of the best mechanical properties. The sinterability of the crystalline alkoxide cordierite powder was highly improved by spark-plasma sintering at a lower sintering temperature (1350 °C), for a very short period of time (7 min). The density of the obtained material was very close to the theoretical density of α-cordierite and the mechanical properties were better than those of materials obtained by conventional sintering.
© 2013 Elsevier Ltd and Techna Group S.r.l. All rights reserved.

Keywords: A. Sintering; A. Sol–gel processes; D. Cordierite

1. Introduction

It is very difficult to obtain dense cordierite ($2MgO \cdot 2Al_2O_3 \cdot 5SiO_2$) ceramics without sintering aids because the difference between the densification and decomposition temperatures of cordierite is very small in the firing process [1]. The main way for an improvement of cordierite sinterability was the synthesis of fine cordierite powders, which can be sintered without sintering aids [2–6]. It was reported that sol–gel cordierite powders are very fine and reactive [3,7–14], but there have not been many systematic investigations concerning the sinterability of such powders [4]. The sintering behavior of commercially available crystalline cordierite powders, which were sintered at temperatures near the incongruent melting point of cordierite (1460 °C), were investigated in several studies [15,16]. Moreover, some researchers [7,17,18] reported that if the densification of pure and homogeneous cordierite powder compact occurs below the crystallization temperature, it could be possible to obtain pure and dense cordierite ceramics with relatively good properties. Therefore, these authors investigated the sinterability of amorphous powders, which were densified by viscous sintering.

In this work, the sinterability of cordierite powders obtained by alkoxide and colloidal sol–gel methods was studied. The sinterability of cordierite powders obtained by gels calcination at a temperature where α-cordierite is formed was compared with the sinterability of powders obtained by gels calcination at a temperature where densification without the onset of crystallization of silica-containing

*Corresponding author.
Tel.: +381 11 3303 721; fax: +381 11 3370 387.
E-mail address: radaab@tmf.bg.ac.rs (R. Petrović).

0272-8842/$ - see front matter © 2013 Elsevier Ltd and Techna Group S.r.l. All rights reserved.
http://dx.doi.org/10.1016/j.ceramint.2012.12.101

compounds occurred. In order to improve sintering behavior of the cordierite powders, spark-plasma sintering (SPS) was applied and results were compared to those obtained by conventional sintering. It is known that SPS allows fast densification, short holding time and low sintering temperatures [19,20]. To the best of our knowledge, spark-plasma sintering has not been previously applied for the sintering of cordierite powders.

2. Materials and methods

2.1. Powders synthesis

Cordierite powders were synthesized by previously published colloidal and alkoxide sol–gel methods [12–14].

Silica sol, boehmite sol, and an aqueous solution of $Mg(NO_3)_2 \cdot 6H_2O$ were used in the colloidal method [12,13].

Silica sol was prepared by using an aqueous solution of sodium silicate, with a mass ratio of SiO_2:Na_2O of 3:1. The solution was diluted to give a solution containing approximately 3.5% SiO_2 and passed through a column filled with a strong acid ion-exchange resin. The effluent solution of polysilicic acid was obtained, which pH value was adjusted by NaOH to approximately 9.2. One part of this solution was heated to boiling in order to form SiO_2 particles and then a rest of the solution was added. The obtained silica sol contained spherical SiO_2 particles of approximately 6 nm.

Boehmite sol was prepared by peptization by HNO_3 of freshly precipitated $Al(OH)_3$, suspended in distilled water. HNO_3 were added at the ratio $n(HNO_3)/n(Al(OH)_3) = 0.1$. Peptization was performed at the boiling point, under reflux during 48 h. The obtained boehmite sol contained rod-like particles of approximately 30 nm in length and about 10 nm in width.

The boehmite and silica sols were mixed and the mixture was stirred for 2 h. Then, an aqueous solution of $Mg(NO_3)_2 \cdot 6H_2O$ was added, and the stirring continued for an additional 2 h. The obtained multicomponent colloidal dispersion was gelled by addition of ammonium carbonate that increased the pH. The resulting gel was dried for two days at 40 °C and then for 24 h at 110 °C.

The alkoxy-derived cordierite gel was synthesized [14] from tetraethylorthosilicate (TEOS), aluminum isopropoxide ($Al(O^iPr)_3$), and magnesium ethoxide ($Mg(OEt)_2$). Ethanol was used as a solvent. The TEOS was partially hydrolyzed for 48 h under reflux at a molar ratio H_2O/TEOS = 1.2 in the presence of HCl as a catalyst, HCl/TEOS = 0.1. A mixture of $Mg(OEt)_2$ and $Al(O^iPr)_3$ in *iso*-butanol was refluxed to form a double alkoxide. After 40 h, the mixture was mixed with partially hydrolyzed TEOS, and again refluxed for 48 h. Water to complete the hydrolysis was added at a molar ratio H_2O/TEOS = 20. The system was left for a week to allow aging of the gel and then dried for 24 h at 110 °C.

Both gels, colloidal and alkoxide-derived, were ground for 0.5 h at 400 rpm in a mill with an alumina chamber using alumina balls.

It was shown previously [12,13] that intensive shrinkage during colloidal gel heating occurred in the temperature range 800–1000 °C. X-ray analysis of the gel calcined at different temperatures showed that spinel crystallized first at about 900 °C and then crystobalite crystallized at temperatures higher than 1000 °C. α-cordierite was formed at about 1300 °C by the reaction of spinel and crystobalite. According to these results, powders for sintering investigation were prepared by the gel calcination at 1300 °C, where α-cordierite is formed, and at 950 °C, where densification without the onset of crystallization of crystobalite occurred.

Intensive shrinkage during heating of alkoxide-derived gel also occurred in the temperature range 800–1000 °C [14]. During thermal treatment of alkoxy-derived gel, μ-cordierite crystallized at 900–1000 °C and in the range from 1100 to 1300 °C transformed into α-cordierite. In order to achieve densification without μ-cordierite crystallization, the gel was calcined at 850 °C, and so obtained powder was used for sintering investigation. The gel was also calcined at 1300 °C in order to obtain crystalline powder for sintering investigation.

All the calcined gels were ground for 3 h at 400 rpm in a mill with an alumina chamber using alumina balls. The obtained powders were designated as $P_{sol}950$, $P_{sol}1300$, $P_{alkoxide}850$ and $P_{alkoxide}1300$, indicating colloidal (P_{sol}) or alkoxide-derived ($P_{alkoxide}$) gel and temperature of calcination (850 °C, 950 °C or 1300 °C). The morphology of the powders was studied by scanning electron microscopy (SEM) using a Jeol JSM-5800 microscope.

The particle size distribution of the powders was determined by a particle size analyzer (PSA) Mastersizer 2000 (Malvern Instruments Ltd., UK). Before determination, the powder was de-agglomerated in an ultrasonic bath (frequency of 40 kHz and power of 50 W), for 1 min.

2.2. Sintering

The cordierite powders were uniaxially pressed at 400 MPa and conventionally sintered at 1400, 1430 and 1450 °C for 2 h.

The powder $P_{alkoxide}1300$ was also sintered by the rapid spark-plasma sintering (SPS) technique in a Dr Sinter SPS System-825C furnace, at 1400 °C for 1 min and at 1350 °C for 7 min. Approximately 3 g of powder were sintered under vacuum using a graphite mold (diameter 20 mm) with an applied pressure of 40 MPa. During sintering, the voltage was 4 V with a current of 1500 A. The required duration of sintering at the desired temperature was determined according the shrinkage of the samples, monitored with a dilatometer. The temperature of the sample during the sintering was measured by an optical pyrometer through a hole located in the graphite mold. After

completion of the process, the samples were cooled for 1 h using the internal cooling system.

The densities of the green compacts and sintered samples were determined by the Archimedes method. The relative densities were calculated using the theoretical density of α-cordierite (2.52 g/cm^3). Microstructures of the fracture surface of the sintered materials were observed by SEM (Jeol JSM-5800). X-ray diffraction analysis of the sintered samples was done using a BRUKER D8 ADVANCE with a Vario 1 focusing primary monochromator (Cu $K_{\alpha 1,2}$ radiation, $\lambda = 1.54059$ Å). The best-sintered materials were polished and used for microhardness (H) and indentation fracture toughness (K_{IC}) determinations. The microhardness was measured with a Vicker's indenter. K_{IC} values were calculated using the formula [21]:

$$K_{IC} = 0.0824 P c^{3/2} \quad (1)$$

where P is the indentation load and c is the length of the induced radial crack. The average of the 20 measurements for each sample was used for the evaluation of the sample hardness and toughness.

After determination of the mechanical properties, the polished conventionally sintered samples were thermally etched at 1350 °C for 30 min, with a heating rate of 20 °C/min, and their microstructure were observed by SEM (JEOL JSM-5800). The spark plasma sintered samples were thermally etched at 1200 °C for 15 min, with a heating rate of 20 °C/min and their microstructure were observed by SEM (TESCAN Mira3 XMU) at 20 kV.

3. Results and discussion

3.1. Powders particle morphology and size distribution

The morphologies of the powders $P_{sol}950$ and $P_{sol}1300$, and $P_{alkoxide}850$ and $P_{alkoxide}1300$ are presented in Figs. 1 and 2, respectively. It could be seen that all the powders had a similar morphology: nearly spherical particles, the dimensions of which were about 0.5 μm, together with larger particles of about 10 μm. Powders particle size distributions based on the particles volume (Fig. 3), show that powders $P_{sol}950$, $P_{sol}1300$, and $P_{alxokside}850$ have a broad and bimodal ditribution, with the maximums at about 2 μm and 20 μm, while the powder $P_{alkoxide}1300$ has a broad and unimodal distribution, enclosing particles in the range of 0.3–20 μm. On the other hand, particle size distributions based on the particles number (data are not shown) showed that particles of 0.5 μm are dominant in all the powders.

Compared to the non-ground powders and those obtained by grinding for 0.5 h [22] (SEM micrographs and particle size distributions are not shown) these powders were much finer.

It was shown previously [23–26] that grinding affects the synthesis and sintering of cordierite. Mechanical treatments of powders have remarkable influence on their reactivity as they promote changes in the texture and structure of the solids. In the case of different raw materials [23–25], increasing of reactivity due to mechanical treatment leads to decreasing of cordierite formation temperature. Also, the grinding of a precursor colloidal gel

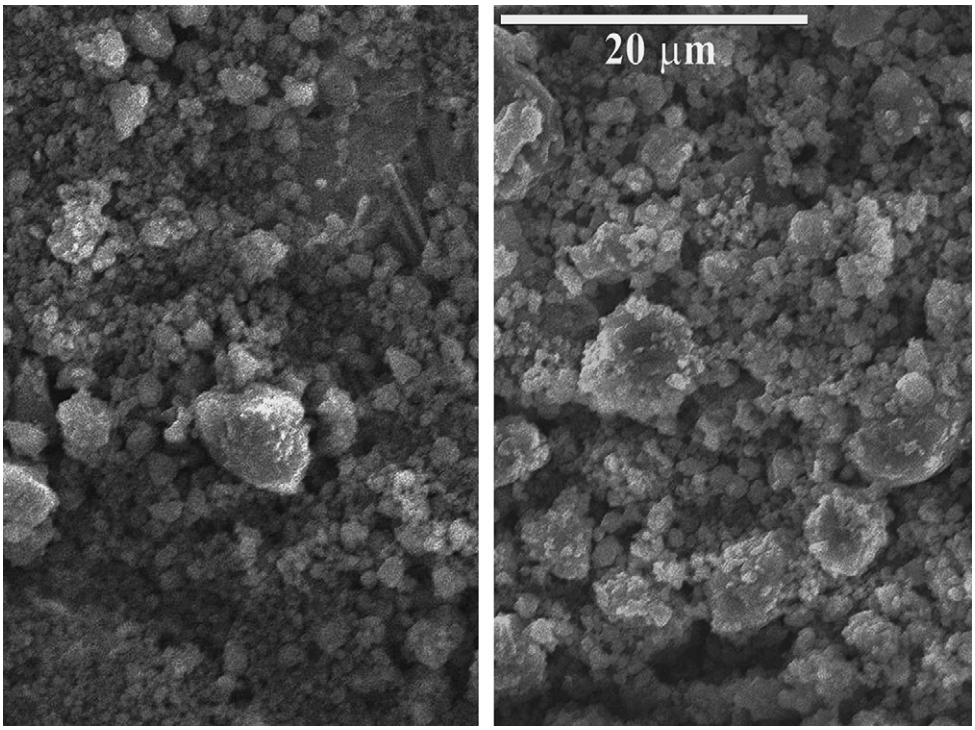

Fig. 1. Morphology of particles of powders: (a) $P_{sol}950$, (b) $P_{sol}1300$.

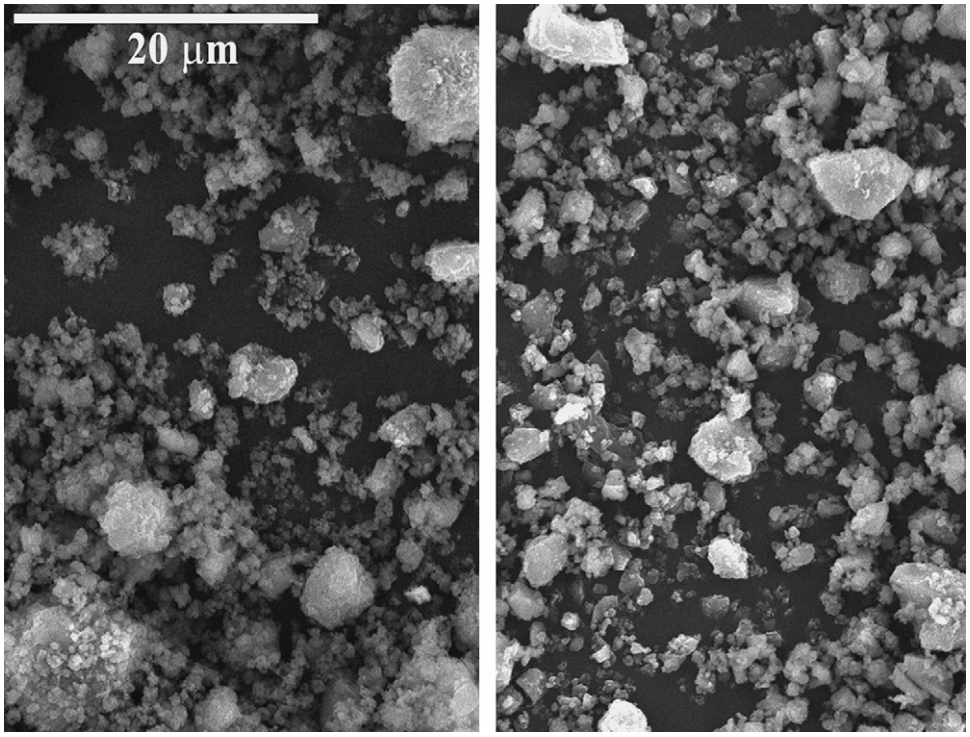

Fig. 2. Morphology of particles of powders: (a) $P_{alkoxide}850$, (b) $P_{alkoxide}1300$.

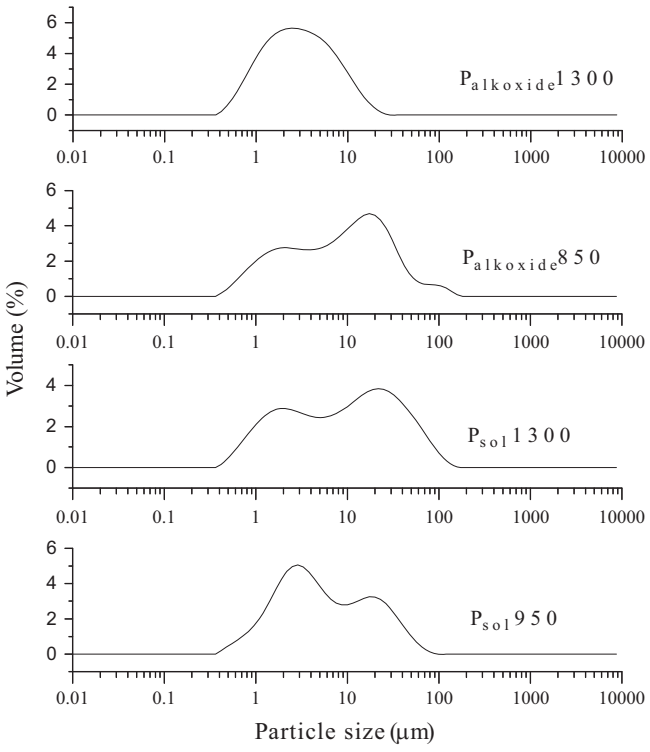

Fig. 3. Particle size distribution of the powders.

[26] promotes the homogeneous distribution of elements in a gel, resulting in improved reactivity for the formation of cordierite. However, in the case of calcined gels, the most important effects of grinding are the particle size decreasing and contribution of accumulated strain energy to the enhancement of diffusion during the sintering process [26].

3.2. Cordierite materials obtained by conventional sintering

3.2.1. Sintering of powders obtained by the colloidal sol–gel method

Microstructures of cordierite materials obtained by conventional sintering of compacts of powders $P_{sol}950$ and $P_{sol}1300$ at 1400 °C are presented in Fig. 4.

The cordierite materials obtained by sintering at 1400 °C are quite dense, with some pores (Fig. 4). By increasing the sintering temperature to 1430 °C, the pores were increased and rounded (SEM micrographs are not presented). The explanation for this could be the beginning of melting, as was seen visually on the samples after sintering. The reason for the decrease in the melting temperature (melting point of cordierite is 1460 °C) could be the presence of Na^+ ions from the silica sol used for synthesis [12,13]. Presence of glasy phase in the materials obtained by $P_{sol}950$ and $P_{sol}1300$ sintering at 1400 °C was not confirmed by X-ray analysis (Fig. 5). Therefore, the optimal sintering temperature for the powders obtained by the colloidal sol–gel method was 1400 °C.

SEM micrographs of polished and thermally etched surface of the cordierite materials obtained by conventional sintering at 1400 °C of the compacts of the powders $P_{sol}950$ and $P_{sol}1300$ are shown in Fig. 6, while the densities (green and after sintering) and mechanical properties of these materials are presented in Table 1.

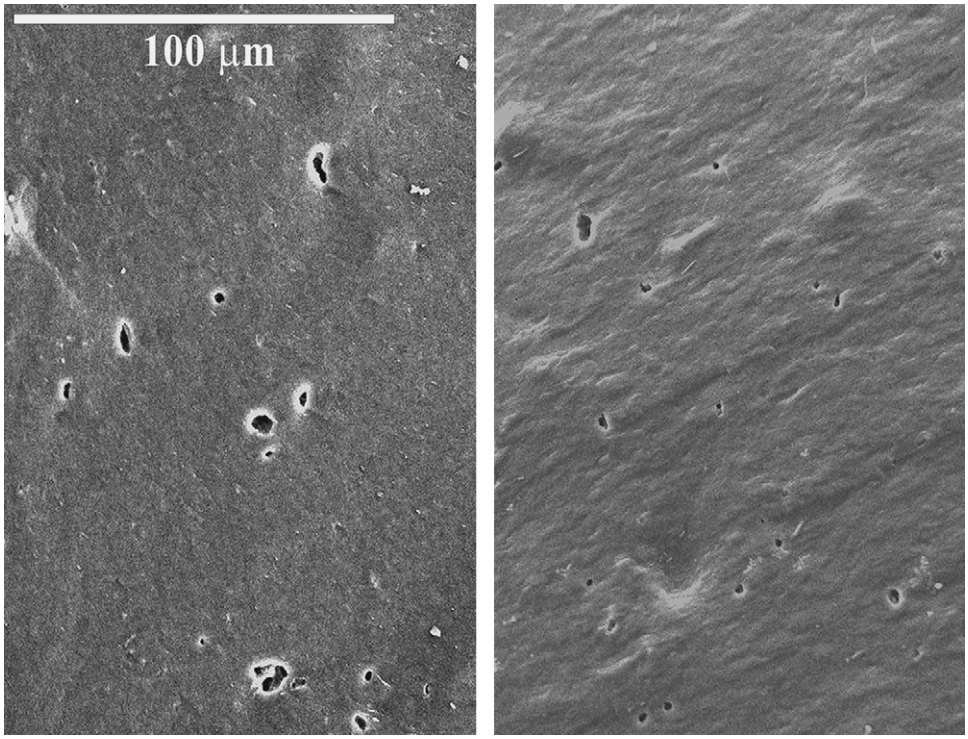

Fig. 4. SEM micrographs of the fracture surface of cordierite materials obtained by conventional sintering at 1400 °C of compact of powder: (a) $P_{sol}950$ and (b) $P_{sol}1300$.

According to Fig. 6, the materials obtained by conventional sintering of the P_{sol} powders at 1400 °C had dense microstructure, with a few small pores. The grain size of the material obtained from powder $P_{sol}950$ seemed smaller than that of the material obtained from powder $P_{sol}1300$. Therefore, a higher value of the fracture toughness of the former material could have been expected than of the latter due to its finer microstructure. However, this was not the case (Table 1). Bearing in mind that powder $P_{sol}950$ was amorphous and that during sintering, crystallization and solid-state reaction occurred, it was assumed that the sintered cordierite materials contained some residual amorphous, glassy phase, the fracture toughness of which is much lower than that of α-cordierite. However, X-ray diffraction analysis of the materials (Fig. 5) showed no presence of glassy phase. Accordingly, lower fracture toughness of the material obtained starting from powder $P_{sol}950$ could be explained by the presence of some microcracks, arising from the thermal mismatch between the different crystalline phases formed during sintering [5]. As stated above, powder $P_{sol}950$ contained spinel and amorphous phase and during thermal treatment, i. e. during sintering, crystobalite crystallized and reacted with spinel, forming α-cordierite.

3.2.2. Sinterability of the alkoxide-based cordierite powders

The microstructures of the cordierite materials obtained by conventional sintering of compacts of powders $P_{alkoxide}$ 850 and $P_{alkoxide}1300$ at 1400 °C are presented in Fig. 7,

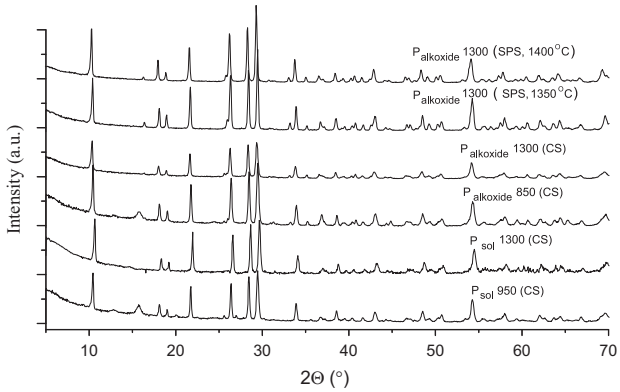

Fig. 5. X-ray diffraction analysis of the materials obtained by conventional sintering (CS) at 1400 °C and spark plasma (SPS) sintering at 1350 and 1400 °C.

while the green densities and densities of sintered materials are presented in Table 1.

According to Fig. 7, the materials obtained by conventional sintering of the $P_{alkoxide}$ powders at 1400 °C were insufficiently sintered. The material obtained by sintering powder $P_{alkoxide}850$ contained densified areas, but both small pores (< 1 μm) and large pores (about 7–8 μm) were present. The dimension of the small pores was approximately equal to the dimension of the smaller particles in the powder $P_{alkoxide}850$ (Fig. 2) and the larger pore size was approximately equal to the size of larger particles. The formation of enclosed nearly spherical pores is indicative of the end of the medium sintering stage and beginning of

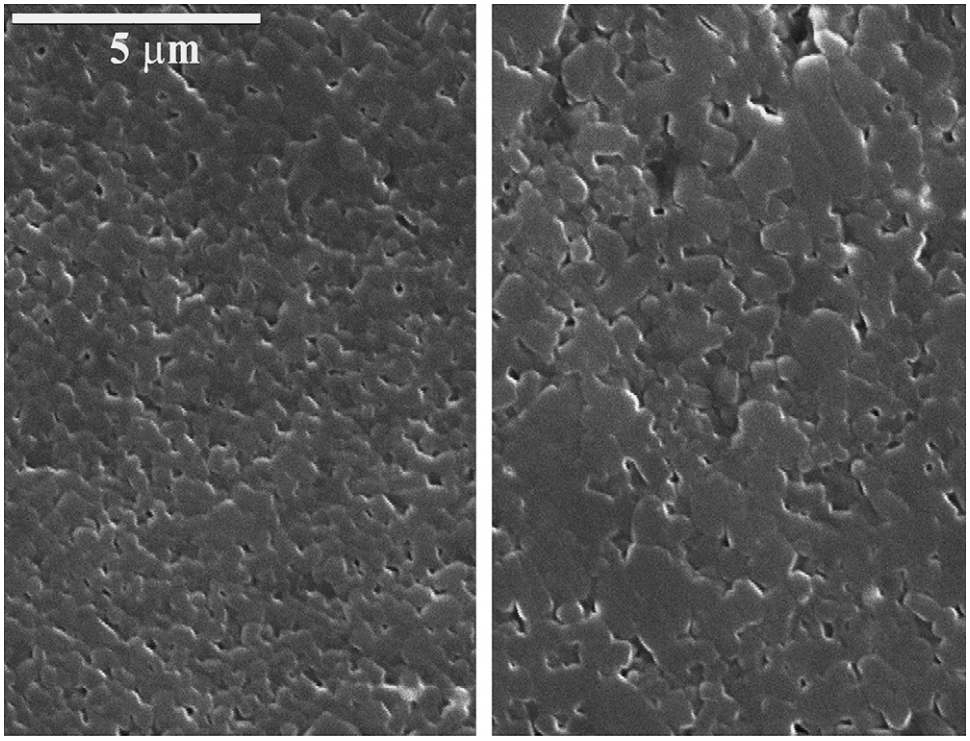

Fig. 6. SEM micrographs of the polished and thermally etched surface of cordierite materials obtained by the conventional sintering at 1400 °C of compacts of powders: (a) $P_{sol}950$ and (b) $P_{sol}1300$.

Table 1
Processing conditions, densities and mechanical properties (hardness and fracture toughness) of cordierite materials obtained by conventional (CS) or spark plasma sintering (SPS).

Type of powder	$P_{sol}950$	$P_{sol}1300$	$P_{alkoxide}850$	$P_{alkoxide}1300$	$P_{alkoxide}1300$	$P_{alkoxide}1300$
Type of sintering	CS	CS	CS	CS	SPS	SPS
Temperature of sintering (°C)	1400	1400	1400	1400	1400	1350
Holding time (min)	120	120	120	120	1	7
Green density (% TD)	66	72	65	70	–	–
Density (% TD)	91	96	88	77	99	99
Hardness (GPa)	8.06	8.05	–	–	8.63	8.53
Fracture toughness (MPa $m^{1/2}$)	2.88	3.67	–	–	4.02	4.06

the final sintering stage. Increasing of sintering temperature (SEM micrographs are not presented) did not cause a decrease in porosity and the material obtained by sintering at 1450 °C contained even more pores, especially small ones, than the material obtained by sintering at 1400 °C. According to some authors [4], such behavior could be explained by swelling and cracking in the compact caused by desorption of the water in the large cavities which connect to form continuous channels parallel to the *c*-axis. They argued that the water concentration of the alkoxy-derived powder would be very high despite powder calcination at high temperatures. The vapor pressure of the water in the cavities or pores could be high enough to expand the cavities or pores and than lead to the cracking of the compact at temperatures above 1400 °C.

An insufficiently sintered sample and the formation of contact necks were the main characteristics of the sample obtained by the sintering of the compact of powder $P_{alkoxide}1300$ at 1400 °C, which means that the sample was in the initial stage of sintering. As the sintering temperature increased, the density of the sample slightly increased and the material obtained by sintering at 1450 °C contained more densified areas (density of the material was approximately 84% TD; SEM micrographs are not presented) than the samples obtained by sintering at 1400 and 1430 °C. However, it could also be the distinct appearance of some large pores, probably because the sintering occurred mainly inside larger agglomerated particles.

X-ray diffractograms of the materials obtained by conventional sintering of compacts of powders $P_{alkoxide}850$ and $P_{alkoxide}1300$ at 1400 °C (Fig. 5) show in both cases presence of well-crystallized α-cordierite, without glassy phase, as in the case of materials obtained starting from P_{sol} powders.

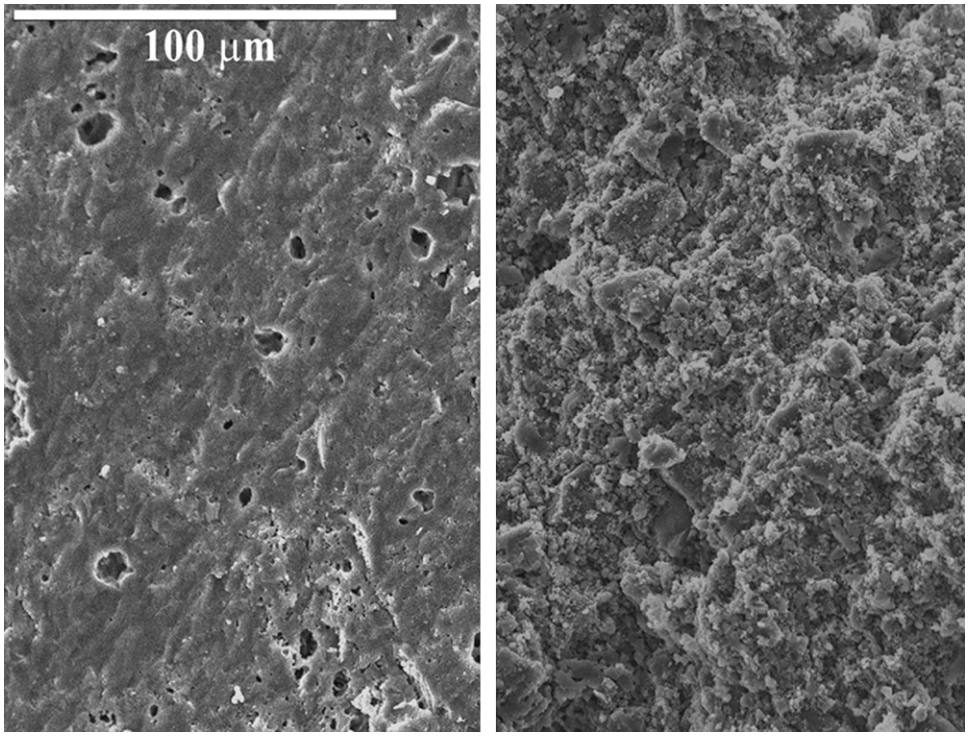

Fig. 7. Microstructure of the cordierite materials obtained by conventional sintering at 1400 °C of powder compacts of: (a) $P_{alkoxide}850$ and (b) $P_{alkoxide}1300$.

Obviously, despite the fact that the sintering temperatures were very close to melting temperature of cordierite, the alkoxide-derived cordierite powders showed very poor performances on sintering, especially the well-crystallized powder $P_{alkoxide}1300$. Despite the fact that powder $P_{alkoxide}1300$ had the same composition (α-cordierite) and similar morphology and particle sizes as the powder $P_{sol}1300$, sinterability of these powders is quite different. It could be supposed that the better performances on sintering of the P_{sol} powders were the results of the presence of Na^+ ions in the silica sol used for the synthesis, which acted as a sintering additive.

Polishing of the materials obtained from the $P_{alkoxide}$ powders was not performed and the mechanical properties were not determined due to the insufficient sintering.

3.3. Cordierite materials obtained by spark-plasma sintering

The microstructures of the cordierite materials obtained by SPS of powder $P_{alkoxide}1300$ at 1350 °C for 7 min and at 1400 °C for 1 min, at different magnifications, are shown in Fig. 8. In both cases, fully densified microstructures were obtained. Pores were rarely observed in either of the specimens. In the higher magnification Figures, no grains can be seen, which indicates that the fracture mode was mainly transgranular.

SEM micrographs of the polished and thermally etched surface of the SPS cordierite materials are shown in Fig. 9, while the densities and mechanical properties of these materials are presented in Table 1. The densities of both materials were very similar to the theoretical value of α-cordierite and the hardness and fracture toughness were very high, higher than of those of the materials obtained by conventional sintering.

Grains of different sizes and shapes and some occasional pores are visible in both microstructures (Fig. 9). In Fig. 9b, two different regions can be seen: one with elongated grains and one with grains that do not look elongated. However, according to the assigned part in Fig. 9b, it could be supposed that both region contained elongated grains, but of different orientation. In the first case, the grains were oriented parallel to polished surface, while in the second case, the grains were oriented perpendicular to the polished surface and a cross section of elongated grains can be seen in the SEM microphotograph. In the case of the sample sintered at 1350 °C for 7 min, elongated grains were also visible on the thermally etched fracture surface (SEM microstructure is not shown).

During spark plasma sintering [27,28], as a consequence of the applied high currents, a softening or melting of the surface layers is possible, leading either to a grain rearrangement by sliding under the applied load or to an enhanced migration of species through the surface layer. The presence of a liquid phase under the applied load could be the reason for the formation of elongated grains. Such a microstructure with elongated grains provides better mechanical properties, especially higher fracture toughness. XRD analysis of SPS materials showed no presence of glassy phase (Fig. 5), which indicates that, even if formed, the content of liquid phase during SPS is very small.

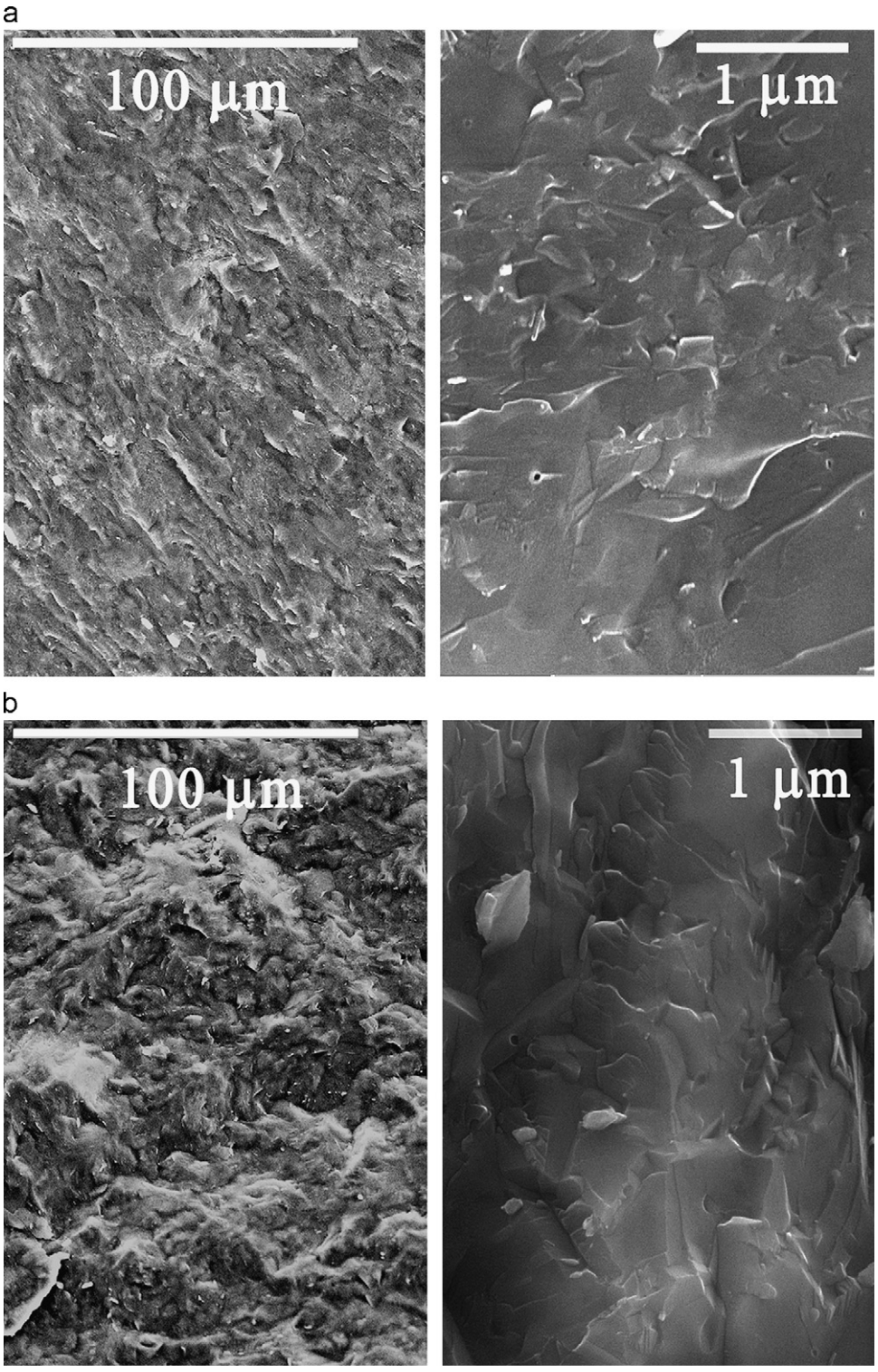

Fig. 8. Microstructure of the cordierite materials obtained by SPS of powder $P_{alkoxide}$1300 at: (a) 1350 °C (7 min), (b) 1400 °C (1 min).

4. Conclusions

In the present study, the sintering behavior of sol–gel processed cordierite powders and the mechanical properties of the obtained cordierite materials were investigated in dependence on the synthesis method, the temperature of gel calcination and the type and temperature of sintering. In general, powders obtained by the colloidal sol–gel method showed better performances on sintering with respect to the alkoxide-based powders. The best

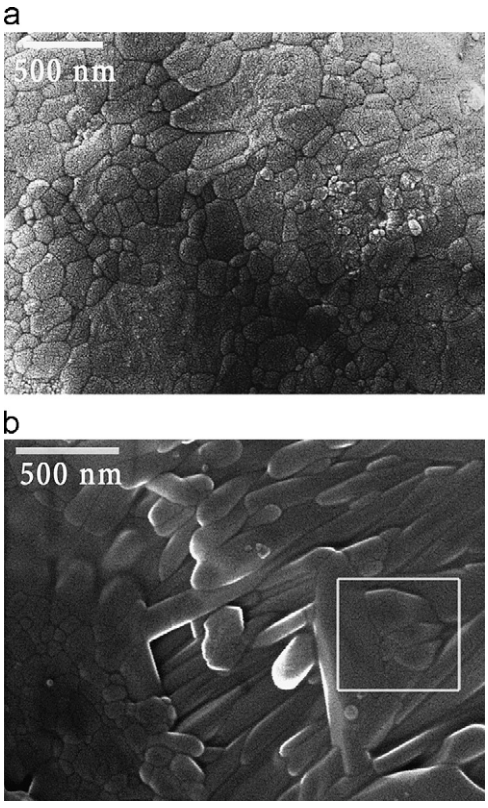

Fig. 9. SEM micrographs of the polished and thermally etched surface of the cordierite materials obtained by SPS at: (a) 1350 °C for 7 min and (b) 1400 °C for 1 min.

mechanical properties of the conventionally sintered materials were achieved by sintering at 1400 °C of powders obtained by colloidal gel calcination at 1300 °C, when α-cordierite was formed. Despite the high sintering temperature of the alkoxide-based powders, the obtained materials were insufficiently sintered. The sinterability of the alkoxide-based powder was highly improved by spark-plasma sintering at a lower sintering temperature and during much shorter time than during conventional sintering. The density of the spark-plasma sintered materials was very close to the theoretical density of α-cordierite and the mechanical properties were better than those of materials obtained by conventional sintering.

Acknowledgments

The authors wish to acknowledge the financial support for this research from the Ministry of Education, Science and Technological Development of the Republic of Serbia through the Project III45019 and FP7-REGPOT-2009-1 NANOTECH FTM, Grant Agreement Number 245916, for financial support for the training of young researchers in the field of spark plasma sintering.

References

[1] J. Hlavač, The Technology of Glass and Ceramics—An Introduction, Elsevier Scientific Publishing Company, Amsterdam, Oxford, New York, 1983.
[2] S.-J.L. Kang, Sintering—Densification, Grain Growth, and Microstructure, Elsevier Butterworth-Heinemann, Oxford, 2005.
[3] H. Suzuki, K. Ota, H. Saito, Preparation of cordierite ceramics from metal alkoxides (Part 1)—preparation and characterization of the powder, Journal of the Ceramic Society of Japan (Yogyo-Kyokai-Shi) 95 (1987) 163–169.
[4] H. Suzuki, K. Ota, H. Saito, Preparation of cordierite ceramics from metal alkoxides (Part 2)—sintering, Journal of the Ceramic Society of Japan (Yogyo-Kyokai-Shi) 95 (1987) 170–175.
[5] H. Suzuki, K. Ota, H. Saito, Mechanical properties of alkoxy-derived cordierite ceramics, Journal of Materials Science 23 (1988) 1534–1538.
[6] Y. Kobayashi, K. Sumi, E. Kato, Preparation of dense cordierite ceramics from magnesium compounds and kaolinite without additives, Ceramics International 26 (2000) 739–743.
[7] A.M. Kazakos, S. Komarneni, R. Roy, Sol–gel processing of cordierite: effect of seeding and optimization of heat treatment, Journal of Materials Research 5 (1990) 1095–1103.
[8] R. Salmon, E. Matijević, Preparation of colloidal magnesium–aluminum–silicates by hydrolysis of a mixed alkoxide, Ceramics International 16 (1990) 157–163.
[9] M.G.M.U. Ismail, H. Tsunatori, Z. Nakai, Preparation of mullite-cordierite composite powders by the sol–gel method: its characteristics and sintering, Journal of the American Ceramic Society 73 (1990) 537–543.
[10] M. Okuyama, T. Fukui, C. Sakurai, Effects of complex precursors on alkoxide-derived cordierite powder, Journal of the American Ceramic Society 75 (1992) 153–160.
[11] M. Awano, H. Takagi, Synthesis of cordierite and cordierite–$ZrSiO_4$ composite by colloidal processing, Journal of Materials Science 29 (1994) 412–418.
[12] R. Petrović, Dj. Janaćković, S. Zec, S. Drmanić, Lj. Kostić-Gvozdenović, Phase-transformation kinetics in triphase cordierite gel, Journal of Materials Research 16 (2001) 451–458.
[13] R. Petrović, Dj. Janaćković, B. Božović, S. Zec, Lj. Kostić-Gvozdenović, Densification and crystallization behaviour of colloidal cordierite-type gel, Journal of the Serbian Chemical Society 66 (2001) 335–343.
[14] R. Petrović, Đ. Janaćković, S. Zec, S. Drmanić, Lj Kostić-Gvozdenović, Crystallyzation behavior of alkoxide-derived cordierite gel, Journal of Sol–Gel Science and Technology 28 (2003) 111–118.
[15] M.A. Camerucci, G. Urretavizcaya, A.L. Cavalieri, Sintering of cordierite based materials, Ceramics International 29 (2003) 159–168.
[16] M.A. Camerucci, G. Urretavizcaya, A.L. Cavalieri, Mechanical behavior of cordierite and cordierite-mullite materials evaluated by indentation techniques, Journal of the European Ceramic Society 21 (2001) 1195–1204.
[17] S.-J. Lee, W.M. Kriven, Crystalliyation and densification of nano-size amorphous cordierite powder prepared by a PVA solution-polymerization route, Journal of the American Ceramic Society 81 (1998) 2605-2612.
[18] H.M. Jang, B.C. Lim, Effects of the scale of precursor mixing on densification behaviors and phase-transformation kinetics of cordierite gels, Journal of Materials Research 9 (1994) 2627–2633.
[19] O. Eser, S. Kurama, A comparison of sintering techniques using different particle sized β-SiAlON powders, Journal of the European Ceramic Society 32 (2012) 1343–1347.
[20] L. An, A. Ito, T. Goto, Effect of sintering temperature on the transparency and mechanical properties of lutetium aluminum garnet fabricated by spark plasma sintering, Journal of the European Ceramic Society 32 (2012) 3097–3102.
[21] A.G. Evans, E.A. Charles, Fracture toughness determinations by indentation, Journal of the American Ceramic Society 59 (1976) 371–372.

[22] N.M. El-Buaishi, I. Janković-Častvan, B. Jokić, Dj. Veljović, Dj. Janaćković, R. Petrović, Sinterability of Cordierite Powders Synthesized by Sol–gel Methods, EUROMAT, C32-P-1-17 (1319), Montpellier, France, 2011, p. 65.
[23] J.B.R. Neto, R. Moreno, Effect of mechanical activation on the rheology and casting performance of caolin/talc/alumina suspensions for manufacturing dense cordierite bodies, Applied Clay Science 38 (2008) 209–218.
[24] E. Yalamac, S. Akkurt, Additive and intensive grinding effects on the synthesis of cordierite, Ceramics International 32 (2006) 825–832.
[25] S. Tamborenea, A.D. Mazzoni, E.F. Aglietti, Mechanochemical activation of minerals on the cordierite synthesis, Thermochimica Acta 411 (2004) 219–224.
[26] M. Awano, H. Takagy, Y. Kuwahara, Grinding effect on the synzhesis and sintering of cordierite, Journal of the American Ceramic Society 75 (1992) 2535–2540.
[27] N. Tamari, T. Tanaka, K. Tanaka, M. Kawahara, M. Tokita, Eifect of spark plasma sintering on densification and mechanical properties of silicon carbide, Journal of the Ceramic Society of Japan 103 (1995) 740–742.
[28] Z.A. Munir, U. Anselmi-Tamburini, M. Ohyanagi, The effect of electric field and pressure on the synthesis and consolidation of materials: a review of the spark plasma sintering method, Journal of Materials Science 41 (2006) 763–777.